On the heating mix of ITER

F. Wagner[1], A. Becoulet[2], R. Budny[3], V. Erckmann[1], D. Farina[4], G. Giruzzi[2], Y. Kamada[5], A. Kaye[6], F. Koechl[7], K. Lackner[1], N. Marushchenko[1], M. Murakami[8], T. Oikawa[9], V. Parail[10], J.M. Park[8], G. Ramponi[4], O. Sauter[11], D. Stork[10], P.R. Thomas[12], Q.M. Tran[11], D. Ward[10], H. Zohm[1], C. Zucca[11]

1) Max-Planck Institut für Plasmaphysik, EURATOM Association, Garching and Greifswald, Germany.
2) CEA, IRFM, F-13108 Saint-Paul-lez-Durance, France.
3) Princeton Plasma Physics Laboratory, Princeton, New Jersey 08543.
4) Istituto di Fisica del Plasma, EURATOM- ENEA-CNR Association, 20125 Milano, Italy.
5) Japan Atomic Energy Research Institute, Naka Fusion Research Establishment, Naka-machi, Naka-gun, Ibaraki-ken 311-01, Japan.
6) Consultant, Oxford OX12 7HA, UK.
7) Association EURATOM-ÖAW/ATI, Atominstitut, TU Wien, Austria.
8) Oak Ridge National Laboratory, Oak Ridge, Tennessee 37831.
9) EFDA Close Support Unit, Boltzmannstrasse 2, D-85748 Garching, Germany.
10) Euratom/CCFE Fusion Association, Culham Science Centre, Abingdon, OX14 3DB, UK.
11) Centre de Recherches en Physique des Plasmas, Association Euratom-Confédération Suisse, EPFL, 1015 Lausanne, Switzerland.
12) FUSION FOR ENERGY, Joint Undertaking, 08019 Barcelona, Spain.

Abstract

This paper considers the heating mix of ITER for the two main scenarios. Presently, 73 MW of absorbed power are foreseen in the mix 20/33/20 for ECH, NBI and ICH. At sufficient edge stability, Q = 10 – the goal of Scenario-2 – seems to be possible with 40 MW of NBI, ICH or ECH. But this goal depends sensitively inter alia on the H-mode pedestal temperature, the density profile shape and on the characteristics of impurity transport. ICH preferentially heats the ions and contributes specifically with $\Delta Q < 1.5$. The success of the Q = 5, steady-state Scenario-4 with reduced current requires discharges with improved confinement necessitating weakly or strongly reversed shear, $f_{bs} > 0.5$, and strong off-axis current drive (CD). The findings presented here are based on revised current drive efficiencies γ for ECCD and a detailed benchmark of several CD codes. With ECCD alone, the goals of Scenario-4 can hardly be reached. Efficient off-axis current drive is only possible with NBI. With beams, inductive discharges with $f_{ni} > 0.8$ can be maintained for 3000 s. The conclusion of this study is that the present heating mix of ITER is appropriate. It provides the necessary actuators to induce in a flexible way the best possible scenarios. The development risks of NBI at 1 MeV can be reduced by operation at 0.85 MeV. NBI is a very important option for steady-state operation of DEMO. For more safety in reaching the H-mode, the addition of 20 MW ECH should be considered.

1. Introduction

Following a request of the European ITER Domestic Agency, F4E, the heating mix of ITER was considered by a study group (AG-2) whose magnetic confinement oriented members and their collaborators are authors of this paper (an earlier EU study is summarized in [1]). The study addressed two ITER scenarios considered in the Project Specification [2]: Q = 10 at 15 MA with a flat-top time of 300 s to 500 s (operational Scenario-2, inductive ELMy H-mode) and Q = 5 at 9 MA under quasi-steady-state conditions (operational Scenario-4). Both scenarios are based on H-mode edge conditions. The nominal power thresholds for Scenario-2 and 4 are 70 MW and 40 MW,

1

respectively. The Q = 10 scenario, with $P_\alpha = 2 P_{ext}$, is based on core heating and mostly inductive current drive (CD). The Q = 5 scenario, with $P_\alpha = P_{ext}$, requires both a high bootstrap current j_{bs} and a CD system with high efficiency γ to allow steady-state operation. The demand on the heating system is therefore to produce a plasma state with steep pressure gradients and to globally drive the plasma current with high efficiency.

The heating mix of ITER as given in the ITER Project Specification [2] is 33 MW NBI (at1 MeV), 20 MW of ECH (170 GHz) and 20 MW of ICH (40-55 MHz). The total power sums up to 73 MW absorbed power. The ITER objectives and the underlying physics is provided by the ITER physics base [3] and its recent update [4] and served as basis for the above mentioned study and this paper. Here, we analyse the ITER performance with respect to its two major goals – Q = 10 and Q = 5, steady-state – for different combinations of heating techniques – NBI, ECH, ICH. Specific issue have been whether ICH could be completely abandoned or to which extent NBI could be replaced by ECH. Various scenarios have been modelled for this study but also already published works of the authors have been included in this paper. Lower hybrid (LH) heating was not investigated but some results from other works will be quoted.

2. Physics background
Operational Scenario-2 is based on strong core heating in order to access a good H-mode. Heating and CD during the current rise are needed to minimize flux consumption by achieving a low internal inductance l_i [5]. At $l_i \approx 0.8$, 30 Vs will remain for the plateau which will allow 400 s burn phase. A bootstrap current fraction $f_{bs} = I_{bs}/I_p \approx 0.2$ is expected.

Scenario-4 aims at large bootstrap and large externally driven currents. Because of the low current drive efficiencies of auxiliary systems current and density are reduced ($I_p = 9$ MA; $n_e = 0.7 \ 10^{20}$ m^{-3}). On the other hand, the plasma confinement time in tokamaks increases with I_p and density. In order to offset the performance reduced by the design parameters, plasmas with improved confinement (HH > 1) have to be developed [i]. This could be achieved with weak or reverse shear q profiles based on the empirical relation that more strongly reversed shear plasmas attain the larger HH factors. Possibly assisted by strong plasma flow a transport barrier develops inside the q-minimum, which - together with the one caused by the H-mode edge pedestal ($\Delta f_{bs}^{edge} \approx 20\%$) - provides the needed level of bootstrap current.

These maximum performance plasmas of Scenario-4 [6] have large β_N [ii] and reside near the operational and stability limits. The stability depends on the pressure peaking factor and the current density profile and has to be improved by additional external measures e.g. to cope with resistive wall modes. As a consequence, there is a strong link between pressure and current density profiles. This is an important difference to Scenario-2, where the pressure profile is predicted to have little direct impact on the q profile and overall plasma performance. As steady-state tokamak scenarios will have density, temperature and q profiles, which are a delicate compromise between taking advantage of local transport improvement and staying within an MHD stable operational domain they are not as well defined and predictable as Scenario-2 and therefore different variants exist. As the bootstrap current is generally much larger than the externally driven current the major goal of a heating method is to serve as actuator providing access to plasmas with good confinement and a high f_{bs}.

---

[i] The factor HH represents the ratio of τ_E to that of the ITER 98(y,2) ELMy H-mode scaling.
[ii] $\beta_N = \beta \ aB/I_p$, with β = volume averaged pressure/magnetic pressure.

This report compares the prospects of different heating and current drive systems employed in a proper mix for ITER and measured on its objectives.
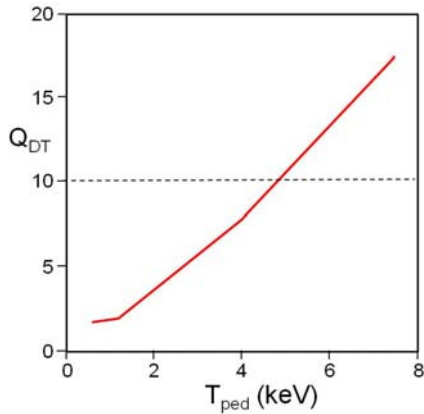

Figure 1. Q_{DT} versus the pedestal temperature T_{ped} for the ITER Scenario-2.

For modelling, transport is taken from the theory-based GLF23 model [7], which reproduces experimental data well. It specifically reproduces the stiff temperature profiles as experimentally observed. In this case, the edge pedestal in the H-mode plays a dominant role because it governs the plasma temperatures over the whole plasma cross-section.

One has to be aware that major uncertainties are introduced by a lack of predictability of fundamental plasma characteristics. Figure 1 shows the relation between Q and the pedestal temperature for Scenario-2 conditions [8]. The external heating is assumed to start at the maximal available power to achieve the H-mode and is then reduced to 47 MW as α-power increases. Q > 10 could only be achieved in a stable way with $T_{ped} \geq 5.2$ keV, which could be the upper limit of realistically expected pedestal temperatures. Unfortunately, there is little theoretical understanding and experimental guidance on the critical gradients and the radial extent of the constituents forming the H-mode edge barrier. In particular, the experimental base on pedestal parameters is specifically poor for heating methods alternative to NBI.

Also particle transport, which defines the density profile shape, is crucial. For ITER flat density profiles are assumed. There is, however, strong experimental evidence that a turbulent convective inward flow in the transport physics of Scenario-2 might peak the density profile toward low collisionality [9]. At peaked n_e, Q would increase by about $\Delta Q > 1$ as long as the core impurity concentration remains unchanged.

It is a robust observation that ECH plasmas at low collisionality are characterised by flat density profiles. This would be less favourable for high Q. ITER has to show with strong α-particle heating whether the dominant electron interaction gives rise to flat n_e profiles. If so, ECH would be a better proxy than NBI, however, with lower Q prospects.

The impurity concentration depends on edge sources and for He on the central one and on the diffusive and convective transport, which could be inward directed. He transport (D_{ash} and v_{ash}) is therefore crucial for high fusion yield. Sensitivity studies have been done in [8].

Only ITER can demonstrate the self-organised plasma characteristics with strong central self-heating by fusion α-particles. In borderline cases, the ΔQ increment from direct ion heating (as provided by ICH: $\Delta Q < 1.5$) could play a role as well as the beam-target fusion interaction as provided by NBI ($\Delta Q \leq 0.5$). Also the impact of sheared rotation as induced by NBI might be beneficial for the creation of an internal transport barrier, ITB, and improved confinement and stability.

3. Current drive modelling
3.1. Electron cyclotron current drive (ECCD)
For an accurate calculation of the current drive efficiency $\gamma = I_{CD} n_e R/P_{CD}$, parallel momentum conservation in the collision processes has to be ensured. The two momentum conserving codes (CQL-3D (Fokker-Planck) [10] and TRAVIS (adjoint technique) [11]) showed consistency in the benchmark. They yield a higher current drive efficiency (for typical ITER applications by ≈ 20%) in comparison to the – at the time of writing - non-conserving approaches (GRAY [12], TORBEAM [13]).

ECH has good core current drive efficiency and excellent localisation of current drive power, which is exploited for MHD stabilisation. For this purpose, dedicated launchers are installed [14]. The EC current drive efficiency drops, however, strongly toward the plasma edge mostly because of the rising fraction of trapped particles; see Fig. 2.
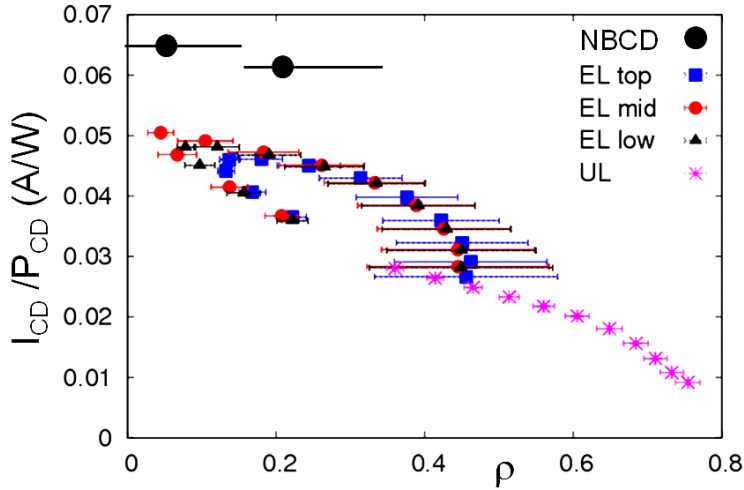

Figure 2. Driven current to CD power versus normalised radius for the ITER $Q = 5$ steady-state scenario (Scenario-4) for NBCD and ECCD utilising the ECH injection options (EL: equatorial launcher; UL: upper launcher). The ECCD calculations are done with momentum conservation (TRAVIS [11]). The horizontal bars indicate the width of the deposition profiles.

3.2. Neutral beam current drive (NBCD)

NBI can drive strong global current arising from the fact that due to $Z_{eff} \neq 1$ and toroidal trapping, the electrons cannot perfectly shield the fast injected ion current. The calculation of the driven current requires the exact description of the ion birth profile due to ionisation and charge exchange and that of the slowing down process. For calculating the fast ion current, multi-step ionisation processes have to be taken into account [15], especially at high energy, necessitating an extension of the initially used cross-sections. Orbit effects are important to describe correctly the location of the driven current. It is therefore important that the magnetic equilibrium is accurately provided to account for the large orbits of the fast ions.

The correct description of the electron shielding requires also precise equilibrium description to get the correct trapped electron fraction. For the beam codes used and benchmarked in this study (OFMC [16] and NUBEAM [17]) differences of about 25% in the current drive efficiency appeared coming mainly from the fast ion current whereas the electron shielding agrees rather well. OFMC calculates an NBI driven current of 2.58 MA and NUBEAM of 2.13 MA, respectively. As the reason for the remaining discrepancies is presently not known both, NUBEAM and OFMC, were used in parallel and the discrepancies were considered as uncertainties.

3.3. Summary on CD modelling

A comparison of CD efficiencies between NBCD and ECCD depends strongly on the conditions prescribed: while for ITER Scenario-2, central ECCD and NBCD efficiency are comparable, off-axis ECCD efficiency is substantially lower than that for NBCD, which - contrary to ECCD - increases with the fraction of trapped particles. This reduction of ECCD necessitates the use of off-axis CD by NBI in Scenario-4 (see Fig. 2).

The physics base for ECCD is quite mature and codes using a fully relativistic momentum conserving approach should give a realistic estimate for the current drive capabilities in ITER. The physics base for NBCD is slightly less developed, with some 25% variation on the modelling side and an unknown fast ion transport that especially affects off-axis CD. The anomalous diffusion of the fast ions does not lead to large discrepancies for central NBCD. Modelling using state-of-the-art codes should therefore be regarded as an upper limit, with the total current at on-axis application being the quantity with the smallest uncertainty.

4. Modelling results

4.1. Scenario-2

Theory-based GLF23 transport model [7], which is used inside the edge barrier, predicts that the plasma density should get peaked in collisionless ITER plasmas. Therefore both imposed flat and self-consistent peaked density profiles are used in the modelling thus defining the performance limits given by the density profile shape. It is assumed in all simulations that transport between top of the edge barrier and the separatrix is reduced to the level which keeps normalised pressure gradient α close to but below the critical level α_{cr}, thus mimicking the limitation by MHD stability. The actual value of α_{cr} was chosen such that the standard case with prescribed flat density profiles and the reference heating mix reached Q = 10. T_e on top of the barrier is 4.6 keV. The width of the edge barrier Δ = 6 cm at the outer mid-plane was kept the same for all cases.

The Scenario-2 plasma cases were simulated with JETTO [18]. Figure 3 summarises the main results of a generic plasma performance study addressing the specifics of the three heating methods and demonstrating the impact of the density profile. The absorbed power is 40 MW for each case, which is the power level sustaining, along with the α-particle heating, a Q = 10 plasma. Peaked density profiles lead to a higher level of fusion gain Q than flat ones with the difference ΔQ > 1 for the case of pure ICH. There is a distinct difference in fusion gain between predominantly ion heating and pure electron heating with ΔQ reaching ΔQ_{max} < 1.5 between ICH and ECH heating. The difference in performance between the reference mix and pure electron heating amounts to ΔQ_{max} < 1.0.
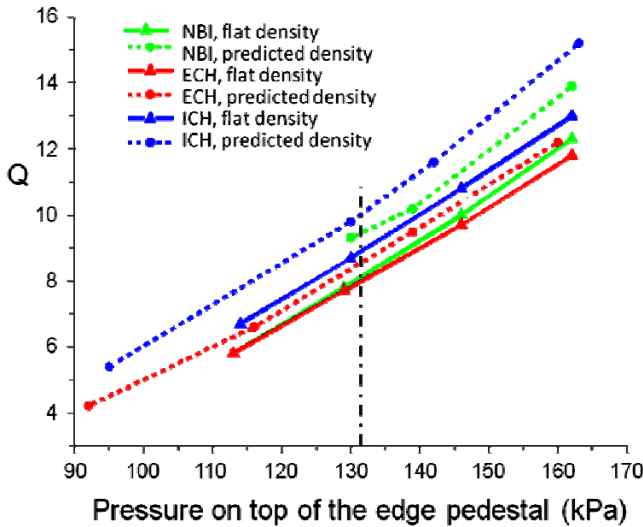

Figure 3. Fusion gain Q for 40 MW of either pure ICH heating (blue lines), pure NNBI with 1 MeV ions (green lines) and pure ECH (red lines) as function of thermal plasma pressure on top of the pedestal. Solid lines correspond to simulations with flat density profiles and dashed lines to peaked densities. The dashed-dotted vertical line is the expected edge pressure stability limit. 6 cm is taken for the barrier width.

Q is plotted in Fig. 3 against the edge pedestal pressure, which, according to the linear MHD stability codes MISHKA[19] and ELITE [20], is limited to p_{ped} < 130 kPa. The limit is indicated in Fig. 3 by the vertical line. The most prominent ITER objective depends critically on MHD stability in a zone with rather involved physics but little predictive understanding. With all reservations it is predicted that ITER may reach Q $\approx$ 10 marginally. Therefore, the proper choice of heating mix is of crucial importance. To stress this is the purpose of this exercise. ITER has better chances to reach its Q = 10 goal with those heating mixes which maximise ion heating (ICH). Scenarios with improved bulk confinement, not considered here, may ease access to Q = 10 if accessible to ITER.

The Scenario-2 flat top time has recently been analysed in detail for different pedestal temperatures and Ejima parameters [21]. In this study here, the reference heating mix was compared with pure ECCD for the volt-second consumption. Both simulations were done under identical assumptions - flat electron density, same α_{crit}. The following conclusions can be drawn: NBI and ECCD have

similar current drive efficiencies (though different profiles). Both methods ($P_{NBI} = 33$MW; $P_{ECH} = 40$MW) generate plasmas with a bootstrap current of $I_{bs} = 3$MA, which is about three times the driven current. Both ECCD and NBCD reduce insignificantly resistive flux consumption (by about 1 Vs per 100 s of burn) and are not expected to play a big role in extending the burn period of Scenario-2. Total resistive flux consumption for the burn phase of Scenario-2 requires approximately 30 Vs for 400 s burn, which is marginally consistent with the capacity of the ITER PF system.

In summary, the exact heating mix is found to be not critical for Scenario-2 and could be NBI, ICH as well as ECH. In any case, ICH should be included to utilise the benefits of direct ion heating.
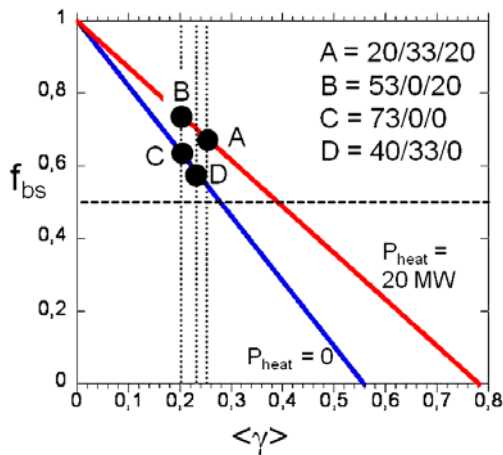
4.2. Scenario-4

Unlike Scenario-2, where the CD characteristics of the heating methods do not critically enter, Scenario-4 was analysed with the help of four distinctly different heating mixes. Heating scenario A represents the baseline ITER mix. All considered cases A-B sum up in to 73 MW absorbed power. Table 1 lists the power mix and the current drive signatures of each case.

Heating Scenario	ECCD				NBCD			ICH	global	
	P (MW)	$\gamma_{CD}(0)$	$\gamma_{CD}(0.4)$	I_{CD} (MA)	P (MW)	γ_{CD}	I_{CD} (MA)	P (MW)	$<\gamma_{CD}>$	f_{CD}
A /20/33/20	20		0.16	0.7	33	0.3	2.3	20	0.25	0.34
B /53/0/20	53	0.22	0.16	2.4	0		0	20	0.2	0.27
C /73/0/0	73	0.22	0.16	3.4	0		0	0	0.2	0.38
D /40/33/0	40	0.22	0.16	1.7	33	0.3	2.3	0	0.23	0.45

Table 1: CD efficiencies γ [10^{20} m^{-2}AW^{-1}], driven currents, the assumed global CD efficiency $<\gamma>$, and the global current drive fraction f_{CD} for the heating scenarios A-D for ITER Scenario-4.

4.2.1. Global considerations

From the definition of $Q = P_{fus}/(P_{heat}+P_{cd})$, the one of $<\gamma>$ and f_{bs} a relation between Q and f_{bs} and, if Q is fixed, one between f_{bs} and $<\gamma>$ can be constructed. P_{heat} is an additional heating power associated with ICH for the heating cases A and B not considered to contribute to current drive. For $Q \approx 5$, f_{bs} is plotted against $<\gamma>$ in Fig. 4 for the two cases $P_{heat} = 0$ and $P_{heat} = 20$MW. The $<\gamma>$ values of the heating scenarios A-D are indicated by vertical lines. For all cases, $f_{bs} > 0.5$ is required.

For ECCD $<\gamma> = 0.22$ (0.16) 10^{20} m^{-2}AW^{-1} for $\rho = 0$ (0.4) (see Table 1). The NBCD efficiency does not vary much with radius and is assumed to be 0.3. ICH is used for central ion heating in scenarios A and B.

With these $<\gamma>$-values, the dependence of Q vs f_{bs} of Fig. 5 is obtained. Scenario D with the highest current drive power reaches $Q \approx 4$ at $f_{bs} \approx 0.5$ and needs $f_{bs} \approx 0.6$ for $Q \approx 5$. Case B without NBCD reaches barely $Q = 3$ at $f_{bs} \approx 0.5$ and requires a much enhanced bootstrap fraction (≈ 0.75) to reach $Q = 5$.

Figure. 4. Plotted is the relation of f_{bs} with $<\gamma>$ for $Q = 5$ for $P_{heat} = 20$ MW and $P_{heat} = 0$. The locations of the four cases A-D (see Table 1) are indicated by dotted lines.

Figure 6 shows the relation between Q and the non-inductive current fraction $f_{ni} = f_{bs} + I_{CD}/I_p$ for $P_{heat} = 0$ and $P_{heat} = 20$ MW (solid and dashed curves). The four reference cases A-D are plotted as solid points. Also variants of A and C were studied. These cases are results of steady state solutions of iterative 1-D transport modeling using GLF23 transport model with existing DIII-D boundary
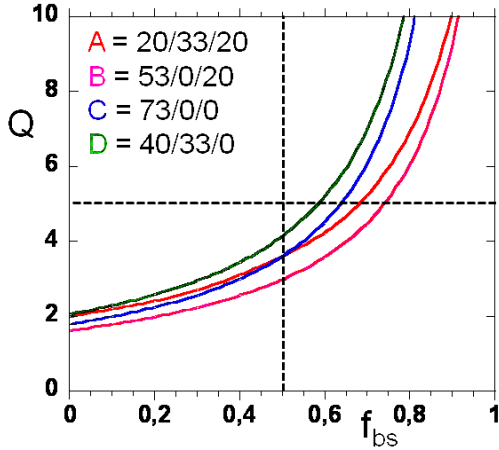
Figure 5. Q versus f_{bs} for the four cases A-D.

information [22]. High Q values are obtained with NBI or ECH, respectively. But only the scenarios with NBCD reach f_{ni} values above 0.8. Direct ion heating provides case B with a higher Q than case C. Detailed simulations around the heating scenarios A and C were carried out. Using NBI and ECRH/ICH in various combinations, which always add up to 73 MW, high f_{ni} and Q ($f_{ni} \approx 0.8$-0.9, $Q \approx 4.5$-5) can be obtained. With ECCD alone, tests have been made using the technical ECCD injection flexibility foreseen at ITER. f_{ni} drops typically below 0.7 and about 2MA are missing, even increasing the ECCD efficiency by 30%. It is obvious that only with NBCD and optimised scenarios can one reach f_{ni} values near 0.9 and Q near 5.

The studies presented here are indicative only and not yet fully optimized. For example better Q values might be obtained with lower power e.g. $P_{ECCD} = 53$ MW instead of 73 MW for the steady-state phase.
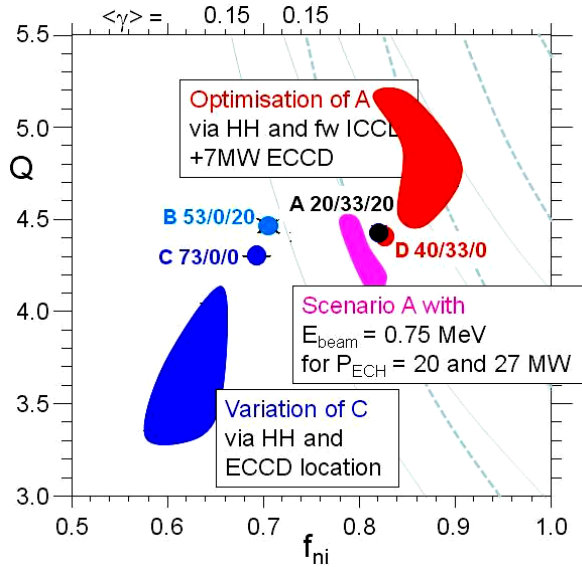

Figure 6. Operational space of Q versus the non-inductive current fraction f_{ni}. Shown are the cases A-D and variants of A and C. For mix A, the consequences of reducing the beam energy to 0.75 MeV was investigated. The curves are based on the simple relation with $f_{bs} = 0.5$ and variable $\langle\gamma\rangle$. The solid curves are with $P_{heat} = 20$ MW, the dashed ones with $P_{heat} = 0$. $\langle\gamma\rangle$ starts with 0.15 and increases in steps of 0.05 up to 0.3 for the 2 cases.

Facing the difficulty with reaching truly steady-state conditions, it is worthwhile to also assess the heating scenarios, which maintain a small inductive current of the order of 1 MA [23] with $f_{ni} < 1$. The ITER baseline heating scenario A has been studied with the GLF23 model and the fast transport code (FastTran), ONETWO and EFIT [24]. These runs have been performed keeping the total plasma current fixed at 9 MA. With an off-axis NBCD set-up, a reduction of f_{bs} by 0.1 compensated by an ohmic contribution of ≈ 1 MA ($f_{ni} \approx 0.9$) $Q \approx 4.5$ can be achieved. These discharges with finite ohmic current will allow ITER to reach the pulse length goal and they will play an important role in the development of steady-state scenarios and the preparation of the steady-state technology.

4.2.2. Modelling of special cases

For the purpose of exploring the virtues of alternative heating mixes, the modelling of special cases refers to the two ITER Scenario-4 reference discharges – type I with strongly reversed magnetic shear in the core and type II with weakly reversed shear (see Fig. 41 in [4]). These two cases represent the operational boundaries toward the strong ITB case with marginally stable q at the plasma centre and the weak ITB case with f_{ni} dropping below 100%. These cases are modelled with HH = 1.37. The reference q and T_e profiles are taken from [25]. If 1-D transport modelling with alternative heating mixes reproduces these target profiles, steady-state performance can be expected.

a) High edge pedestal temperature

7

With the assumption of a high edge pedestal ($T_{ped} > 7keV$) leading to a high edge bootstrap current contribution, stationarity is obtained with the non-inductive fraction, f_{ni}, even in excess of 100%; f_{bs} = 0.7, Q = 5.3, and β_N = 3.1 [26]. In the ONETWO code modelling NBI and ECCD were used for current drive and ICH for central heating. The transport model used is GLF23 without an ITB being developed. The NBI and ECCD power deposition profiles used in these simulations are all off-axis, with NBCD contributing specifically to the I_{CD}.

b) High internal transport barrier

In this case weakly or strongly reversed q-profiles have to be tailored and sustained. $q(\rho)$ and $\chi(\rho)$ profile need to be consistent. It has been verified that there is the technical flexibility at ITER to correspondingly shape the q-profile by ECCD. With the improved equatorial launcher (EL) having one row in counter-CD, the necessary q profiles – zero shear, weakly and strongly reversed shear - can be produced and controlled under conditions close to the ITER reference scenarios [27].
In a sensitivity study a weak shear case was explored in detail with 50 MW of NBI and 20 MW of ECCD. HH was assumed to be 1.37. $f_{bs} \approx 0.5$ without a high temperature pedestal. At I_p = 8.5MA Q = 5 was achieved steady state.

c) Case with ECCD alone

ECCD with P_{CD} = 50 MW and 70 MW were studied. Without NBCD, the total current drops down to 6 MA causing a serious reduction in performance. Q depends significantly on I_p ($\sim I_p^3$). 50 MW yields higher Q values than 70 MW. This is because the increase in I_{ECCD} does not offset the increase in auxiliary power, due to the low average CD efficiency. 50 MW ECCD yield Q $\approx$ 3 with HH = 1.37 [28]. One way of compensation is by increasing the HH factor (and scaling thereby the effective $\chi(\rho)$). Again in the spirit of a sensitivity study HH has been varied between 1.3 and 1.78. Even for the highest HH factor the performance losses due to the lower total plasma current are not recovered. No steady-state scenarios are found with $f_{ni} > 0.85$ and Q near 5 with ECCD only or with ECCD and ICCD.

d) Doubling the core ECCD current drive efficiency

This case represents a further sensitivity study where γ was increased by a factor 2 in the core where temperatures are highest and trapped particle fraction smallest. At the edge, there is no enhancement because the linear predictions are considered to be relevant. Even with this optimistic assumption and HH = 1.78, $I_{ECCD} < 3MA$, $I_p \approx 7MA$ and Q just below 5 are obtained. The strategy to maximize the driven current while q is kept above 1 leads to a current profile clearly too peaked and not compatible with HH = 1.78.

e) LH and NBCD

Steady-state profiles have been obtained with weak and strongly reversed shear with 33 MW of NBI and 34 MW of LHCD at an HH factor of 1.37. Q = 5 at I_p = 9 MA is achieved with profiles similar to the ITER reference ones. The current density profile for LHCD is taken from [29]. However, the LHCD efficiency of 0.3 $AW^{-1}10^{20}m^{-2}$ is now considered as too optimistic, since the type of antennas compatible with the ITER environment [30] (Passive-Active Multijunction) do not exceed directivities of 70 %. Efficiencies of the order of 0.2 $AW^{-1}10^{20}m^{-2}$ are considered as more realistic. Moreover, it is neither likely that 30 MW of LH power could be launched from a single ITER port, nor that two ports will be available [28]. Therefore, an injected LH power limited to 20 MW, with a 70 % directivity should be considered as the reference operation value.

f) LHCD, ICRH and ECCD

For this RF-only case [31] current density maxima of j_{bs} and j_{ECCD} coincide at $\rho = 0.45$. Here an ITB develops, which is triggered and locked by ECCD. The LHCD power deposition is located at

$\rho = 0.7$ and the current drive obtained (≈ 0.6 MA) contributes to the total non-inductive current fraction ($f_{ni} \approx 0.97$). ICH provides central heating. Currents driven inside the ITB have been found to lead to shrinking and final collapse of the ITB itself [29]. This is the well known problem of current alignment, i.e. an incompatibility of the profiles of non-inductively driven and bootstrap current that prevents steady-state profiles to be sustained [32]. The details depend, however, on the transport model relating shear and χ. With this current drive scheme, the q profile obtained is stable for 1000 s at $I_p = 8$ MA, with $q_0 \approx 6$ and $q_{min} > 2$. Q = 6.5 is obtained. This scenario is, however, rather demanding in terms of MHD. Owing to the strongly negative shear combined with large pressure gradients, theses plasmas are prone to resistive interchange modes [31].

h) Cyclic operation

A cyclic scenario has been recently developed [33] where the heating and current drive power varies between a phase with inductive current drive and a phase where the transformer is recharged. The average flux consumption in a complete cycle is zero, the average fusion power is 375 MW, and Q about 6.2. The heating mix for the first phase is NBI/IC/LH/EC = 0/20/15/17 MW. ICH and LHCD are used to provide central heating and non-inductive CD, respectively; ECCD sustains an ITB under weak shear conditions. The heating mix for the transformer recovery phase is NBI/IC/LH/EC = 33/8/15/11.5 MW. Strong NBCD is necessary in this phase. This example shows that 3000 s operation in ITER can be conceived as a combination of various scenarios. The long resistive time constant is used to be able to recover the ITB and the good performance phase when the NBCD is turned off.

5. Considerations regarding CD technology

5.1. NBI

High-power NNBI at 1 MeV energy requires extensive R&D. Such ion-sources are not yet available, the R&D costs and the system costs are high and the time schedule is challenging. Because of the considerable risks the use of 0.85 MeV instead of 1MeV beam energy has been considered as risk mitigation. The modelling, done with different code packages, indicates that such a reduction of the beam energy reduces the current drive efficiency by less than 20%. This is acceptable if the overall power is maintained at the 33 MW level. This can be achieved by operating at increased current density from the ion source, by reducing the losses in the injector and the NB duct, or a combination of those parameters. At a beamlet divergence ≈ 5 mrad, as already operated at the prototype accelerator at JAEA, a beam energy of only ≈ 0.85 MeV would provide 16.5 MW injected into ITER. Improvements in current density up to 30% can realistically be expected, but the co-extracted electron current must be controlled. The reduction in beam energy would not affect the goals of Scenario-2; the decrease of current drive efficiency for Scenario-4 (see Fig. 6 for 0.75 MeV beam energy) can be compensated with ECCD or – more speculatively - via a higher bootstrap current arising from the increased torque at lower beam energy improving confinement.

Considering the substantial effort required a critical issue is whether NNBI can also drive the current required for DEMO. DEMO can be heated without NBI and steady state current drive can be achieved with ECCD. However, the increased CD power required in this case necessitates an enlargement of the unit size to deliver the same output. This leads to an increase of perhaps 25% both in the capital and the electricity costs, the cost driving factor being the recirculating power for CD [34]. Whereas a steady state DEMO with NBI needs a CD power of about 200 MW, it will need twice that power with ECCD. The R&D for the NBI system should therefore remain targeted for 1MeV beam energy, which will – considering also DEMO - reduce the overall development costs. It seems that a decision against NBI on ITER risks removing an important option for steady-state operation of DEMO.

5.2 ECH

There is sufficient know-how and capacity across the ITER partners to ensure timely delivery of gyrotrons with at least 1 MW unit output. The overall R&D risks are mitigated because ITER-like systems are well advanced for W7-X [35]. The use of diplexers or gyrotrons with higher power (> 1MW) would allow the full exploitation of the foreseen transmission and launching systems, to reduce the space demand, number of transmission lines, and system complexity in close neighbourhood of the device, and thus also to substantially reduce the marginal cost of a power enhancement [36]. A future enhancement in ECH power up to a total of 40 MW is recommended to increase the operating margins across the scenarios. If agreed in a timely manner, this would also mitigate the technical development risks of NNBI (e.g. in case the full power is not reached at lower voltage).

5.3. ICH

ICH is the heating method with the lowest costs. Experience with the operation of the ITER-like ICH antenna on JET reduces the development risks of this heating system [37]. Nonetheless, the coupling depends on the plasma density in the outer scrape-off layer which is not well known. ICH is different to the other heating mechanisms because prior knowledge of plasma properties is necessary for precise coupling predictions. The installation of two antennae (for a total of 20 MW coupled power) in the early hydrogen and deuterium phases of the project will better ensure the timely availability of sufficient additional heating power.

5.4. LH

LH has not been studied in detail here. The advantage of LH is in uniquely providing large γ in the plasma periphery, which would facilitate the achievement of Scenario-4. Its disadvantage is that the wave coupling depends on edge plasma properties, which are not known at present. Because of the criticality of Scenario-4 it is recommended to add LH, but only after operational experience has been gained. This will only be possible with timely implementation of the necessary R&D.

6. Conclusions and summary

The presently foreseen heating mix A seems to best ensure the accessibility to the full range of ITER operation scenarios whilst providing the flexibility required for an experimental device. The heating mix seems to be uncritical for Scenario-2. ICH and a peaked density profile would support the development of Q = 10. Critical seems to be the edge temperature pedestal and the edge pressure gradient. H-mode versions with improved core confinement – not considered in this study – could overcome possible limitations of the baseline scenario.

Scenario-4 clearly needs in-situ development and will be part of the experimental programme of ITER. For its success, a flexible heating system is necessary. Secondary characteristics of the various methods can be utilised as actuators to induce specific plasma responses. Owing to the limitations in the CD efficiencies of the presently foreseen systems, LH should be considered for a later experimental stage.

NBI seems to be indispensable due to the high off-axis current drive efficiency. The technical development risks with beam energies up to 1 MeV are high, however. A lower beam energy target of 0.85 MeV would be acceptable for ITER. For the DEMO needs the NNBI R&D should, however, target for 1 MeV beams. ECH is technically mature in the present frequency range. Its off-axis CD efficiency is too low, however, to serve as exclusive current drive method.

ITER will be limited to Q ≈ 2-3 if the H-mode is not achieved. The DT power threshold for ITER plateau conditions is about 70 MW (40 MW) for Scenario-2 (Scenario-4). Furthermore, high confinement H-modes will require a power typically 20 % above threshold. This compares with 73 MW of external heating and ≈ 40 MW of P_α in the L-mode of Scenario-2 settings just prior to the

H-transition. The power margin for Scenario-2 is critical and is much smaller than for any of the experiments, which prepared the data basis for ITER. Hydrogen or helium plasmas foreseen for the early phases will have even higher H-mode thresholds. It is therefore suggested to increase this power margin at ITER by additional 20 MW of ECH.

Acknowledgement

References

[1] R. Wilhelm, Plasma Phys. Contr. Fusion **40** (1998) A1.
[2] Progress in the ITER Physics Basis, Nucl. Fusion **47** (2007).
[3] ITER Physics Base, Nucl. Fusion **39** (1999) 2521.
[4] ITER Physics Base Update, Nucl. Fusion **47** (2007) S301.
[5] A.C.Sips et al.,22nd IAEA Fusion Energy Conf., paper IAEA-CN-165/IT/2-2
[6] Progress in the ITER Physics Basis, Nucl. Fusion **47** (2007) S285.
[7] R.W. Waltz, *et al.,* Phys. Plasmas **4** (1997) 2482.; and http://w3.pppl.gov/NTCC/GLF
[8] R. V. Budny, Nucl. Fusion **49** (2009) 085008.
[9] C. Angioni et al., Phys. Rev. Lett. **90** (2003) 205003.
[10] R. W. Harvey and M. G. McCoy, in Proc. IAEA Tech. Comm. Meeting 1992 (IAEA, Vienna, 1993), p. 498.
[11] N. Marushchenko et al., Nucl. Fusion **48** (2008) 054002.
    N. Marushchenko et al., Nucl. Fusion **49** (2009) 129801.
[12] A.V. Zvonkov et al., Plasma Phys. Rep. **24** (1998) 389.
    D. Farina, *Fusion Science & Technology* **52,** 154 (2007)
[13] E. Poly, G.V. Pereverzev and A.G. Peeters, Phys. Plasmas **6** (1999) 5.
[14] G. Ramponi et al., Fusion Engin. Design **82** (2007) 454.
[15] T. Oikawa et al., Nucl. Fusion **41** (2001) 1575.
[16] M. Tuszewiski and J.P. Roubin, Nucl. Fusion **28** (1988) 499.
[17] A. Pankin et al., Comput. Phys. Commun. **43** (1981) 61.
[18] G. Cenacchi and A. Taroni, in Proc. 8th Comput. Physics, Computing in Plasma Physics, Eibsee, 1986; European Physical Society, Petit-Lancy, 1986, Vol. 10D, p. 57.
[19] A. B. Mikhailovskii et al., Plasma Phys. Rep **23** (1997).
[20] P. B. Snyder et al., Phys. Plasmas **9** (2002) 2037.
[21] C. E. Kessel et al., Nucl. Fusion **49** (2009) 085034.
[22] J.M. Park et al., 3rd ITPA IOS TG meeting (Frascati, 2009) to be submitted to Nucl. Fusion.
[23] R. V. Budny, Phys. of Plasmas **17** (2010) 042506.
[24] H. St. John et al., in Proc. Conf. Contr. Fusion and Pl. Phys., Lisboa, 1993 (Europ. Phys. Soc, Geneva, 1993) Vol. I, p.99.
[25] C. Gormezano et al., Nucl. Fusion **47** (2007) 285.
[26] G. Giruzzi *et al*, 21st IAEA Fus. Energy Conf. (2008), paper IT/P6-4.
[27] C. Zucca, 2009 *PhD Thesis* EPFL, no 4360 http://library.epfl.ch/en/theses/?nr=4360.
[28] O. Sauter and C. Zucca, *On the Role of Heating and Current Drive Sources on the Scenario 4 for ITER: preliminary results with EC only* (June 2009), report.
[29] Bonoli P.T. *et al* 2006 *Proc. 21st Int. Conf. on Fusion Energy 2006 (Chengdu, China, 2006)* (Vienna: IAEA) CD-ROM file IT/P1-2.
[30] G.T. Hoang et al., Nucl. Fusion **49** (2009) 075001.
[31] J. Garcia *et al*, Phys. Rev. Lett. **100** (2008) 255004.
[32] J. Garcia and G. Giruzzi, Phys. Rev. Lett. **104** (2010) 205003.
[33] J. Garcia et al., Nucl. Fusion **50** (2010) 025025.
[34] D. Ward, presented at this conference; to be published in Plasma Phys. Contr. Fusion.
[35] V. Erckmann, *et al.*, Fusion Science and Technology **52** (2007) 291.
[36] V. Erckmann, et al., Fusion Science and Technology **55** (2009) 23.
[37] M. P. S. Nightingale et al., Radio Frequency Power in Plasmas, AIP Conference Proceedings 1187, eds. Bobkov & Noterdaeme, 2009, p.213.